Protein Science (1999), *8*:1816–1824. Cambridge University Press. Printed in the USA.
Copyright © 1999 The Protein Society

Functional analyses of AmpC β-lactamase through differential stability

BETH M. BEADLE, SUSAN L. McGOVERN, ALEXANDRA PATERA, AND BRIAN K. SHOICHET

Department of Molecular Pharmacology & Biological Chemistry, Northwestern University, 303 E. Chicago Avenue, Chicago, Illinois 60611-3008

(RECEIVED March 15, 1999; ACCEPTED May 26, 1999)

Abstract

Despite decades of intense study, the complementarity of β-lactams for β-lactamases and penicillin binding proteins is poorly understood. For most of these enzymes, β-lactam binding involves rapid formation of a covalent intermediate. This makes measuring the equilibrium between bound and free β-lactam difficult, effectively precluding measurement of the interaction energy between the ligand and the enzyme. Here, we explore the energetic complementarity of β-lactams for the β-lactamase AmpC through reversible denaturation of adducts of the enzyme with β-lactams. AmpC from *Escherichia coli* was reversibly denatured by temperature in a two-state manner with a temperature of melting (T_m) of 54.6 °C and a van't Hoff enthalpy of unfolding (ΔH_{VH}) of 182 kcal/mol. Solvent denaturation gave a Gibbs free energy of unfolding in the absence of denaturant ($\Delta G_u^{H_2O}$) of 14.0 kcal/mol. Ligand binding perturbed the stability of the enzyme. The penicillin cloxacillin stabilized AmpC by 3.2 kcal/mol ($\Delta T_m = +5.8$ °C); the monobactam aztreonam stabilized the enzyme by 2.7 kcal/mol ($\Delta T_m = +4.9$ °C). Both acylating inhibitors complement the active site. Surprisingly, the oxacephem moxalactam and the carbapenem imipenem both destabilized AmpC, by 1.8 kcal/mol ($\Delta T_m = -3.2$ °C) and 0.7 kcal/mol ($\Delta T_m = -1.2$ °C), respectively. These β-lactams, which share nonhydrogen substituents in the 6(7)α position of the β-lactam ring, make unfavorable noncovalent interactions with the enzyme. Complexes of AmpC with transition state analog inhibitors were also reversibly denatured; both benzo(b)thiophene-2-boronic acid (BZBTH2B) and p-nitrophenyl phenylphosphonate (PNPP) stabilized AmpC. Finally, a catalytically inactive mutant of AmpC, Y150F, was reversibly denatured. It was 0.7 kcal/mol ($\Delta T_m = -1.3$ °C) less stable than wild-type (WT) by thermal denaturation. Both the cloxacillin and the moxalactam adducts with Y150F were significantly destabilized relative to their WT counterparts, suggesting that this residue plays a role in recognizing the acylated intermediate of the β-lactamase reaction. Reversible denaturation allows for energetic analyses of the complementarity of AmpC for β-lactams, through ligand binding, and for itself, through residue substitution. Reversible denaturation may be a useful way to study ligand complementarity to other β-lactam binding proteins as well.

Keywords: β-lactam; β-lactamase; AmpC; denaturation; enzyme stability; penicillin binding protein; protein stability

The interactions of β-lactams with β-lactamases and penicillin binding proteins (PBPs) have been studied intensely for decades (Strominger & Tipper, 1965; Hall & Knowles, 1976; Fisher et al., 1980; Ishiguro et al., 1997; Li et al., 1997). Not only are these proteins medically important, they are, in many ways, model enzymes; this is especially true of β-lactamases (Hall & Knowles, 1976; Christensen et al., 1990). Consequently, many mechanistic aspects of β-lactamases and PBPs are well understood. Paradoxically, little is known about the energies of binding of β-lactams to these cognate enzymes.

Our ignorance of the energies of binding of β-lactams to serine β-lactamases and PBPs is a consequence of their mechanism of binding. The first encounter complex between a β-lactam and the enzyme is rapidly transformed into an acyl adduct by nucleophilic attack of the catalytic serine on the electrophilic lactam carbonyl carbon (Fig. 1). Measuring the equilibrium between the bound and free β-lactam is thus difficult. This effectively precludes measuring binding affinity by standard techniques, since affinity can only be determined at equilibrium. For β-lactams binding to β-lactamases and PBPs, Ki values are only apparent; the true binding constants are unknown.

Reprint requests to: Brian K. Shoichet, Department of Molecular Pharmacology & Biological Chemistry, Northwestern University, 303 E. Chicago Avenue, Chicago, Illinois 60611-3008; e-mail: b-shoichet@nwu.edu.

Abbreviations: ΔC_p, change in heat capacity at constant pressure; ΔG_u, Gibbs free energy of unfolding; $\Delta G_u^{H_2O}$, Gibbs free energy of unfolding in the absence of denaturant; ΔH_{VH}, van't Hoff enthalpy of unfolding; ΔS_u, entropy of unfolding; BZBTH2B, benzo(b)thiophene-2-boronic acid; C_m, midpoint concentration; CD, circular dichroism; Gdn·HCl, guanidinium hydrochloride; PBP, penicillin binding protein; PNPP, p-nitrophenyl phenylphosphonate; T_m, temperature of melting; UV, ultraviolet; WT, wild-type.

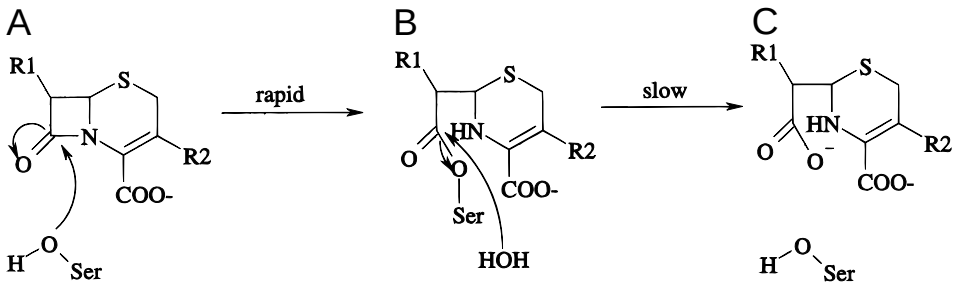

Fig. 1. Simplified mechanism of AmpC β-lactamase. **A:** Ser64 of AmpC attacks the carbonyl carbon of the intact β-lactam antibiotic. **B:** The acyl intermediate. **C:** The hydrolyzed β-lactam antibiotic and the regenerated AmpC enzyme.

Differential protein stability can measure the thermodynamic complementarity of a ligand for an enzyme and does not depend on measuring the equilibrium between bound and free ligand (Schellman, 1976). The binding of a ligand to an enzyme will perturb the stability of that enzyme to denaturation, typically by stabilizing it. The stability difference between the saturated ligand-enzyme complex and the enzyme alone quantitatively measures the noncovalent energetic complementarity between ligand and enzyme (Morton & Matthews, 1995). Rather than measuring the equilibrium between bound and free ligand, this involves measuring the equilibrium between the folded and unfolded forms of both the free enzyme and the enzyme adduct (Fig. 2). This technique is reliable as long as denaturation is reversible and two-state, and the interaction between the adduct and the unfolded protein is negligible. Indeed, similar denaturation studies were used to measure the complementarity of transition state analogs for a class A β-lactamase (Rahil & Pratt, 1994). Although denaturation was not reversible in this system, the increases in the temperatures of melting correlated with the expected binding energies.

Reversible denaturation seems well-suited for studying the thermodynamic complementarity between a β-lactamase and a β-lactam. Since denaturation does not break covalent bonds, the differential energy of unfolding between a β-lactam-bound enzyme and the apo-enzyme reflects the noncovalent interaction energy between the enzyme and the β-lactam. The differential stability between the apo- and β-lactam-bound enzyme has the same sense as the differential stability between a wild-type and a mutant enzyme—both reflect differential noncovalent interactions.

Here, we investigate the reversible denaturation of the class C β-lactamase AmpC. We compare the thermodynamic unfolding of the WT enzyme to the unfolding of its adducts with several β-lactams and also transition state analogs (Fig. 3). This allows us to determine differential energies of unfolding ($\Delta\Delta G_u$) and hence the energetic complementarity of these ligands for the enzyme. We also investigate the effects of mutation of a key catalytic residue on the internal stability of the enzyme and on its function. Unexpectedly, we find that the well known β-lactams moxalactam and imipenem destabilize AmpC on complex formation. Such destabilization has surprising implications for enzyme-substrate recognition in this highly studied system.

Results

Two-state, reversible thermal denaturation of AmpC and AmpC Y150F

AmpC was denatured by temperature in 50 mM KPi, 200 mM KCl, 38% ethylene glycol, pH 6.8, as monitored by far-UV CD (Fig. 4A). The melting behavior was fit using a two-state analysis program (Kirchhoff, 1993) to give an average T_m of 54.6 °C and an average ΔH_{VH} of 182 kcal/mol at a ramp rate of 2 °C/min (Table 1).

To interpret melting thermodynamically, it is important to determine the reversibility and two-state behavior of the protein. After thermal denaturation of AmpC, the sample was immediately cooled; 91% of the folded CD signal returned. The β-lactamase activity against the cephalosporin cephalothin prior to denaturation was equal to the activity after renaturation. Both experiments indicate that the thermal denaturation of AmpC is reversible.

To determine whether the melting of AmpC could be described as two-state, we compared the denaturation monitored by CD at 223 nm, which measures secondary structure, to the denaturation

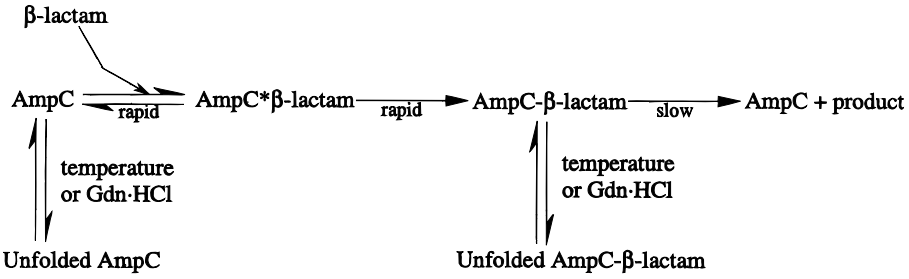

Fig. 2. Measuring β-lactam binding affinity for AmpC by differential stability. The AmpC∗β-lactam represents the first encounter complex; the AmpC-β-lactam represents the acyl adduct.

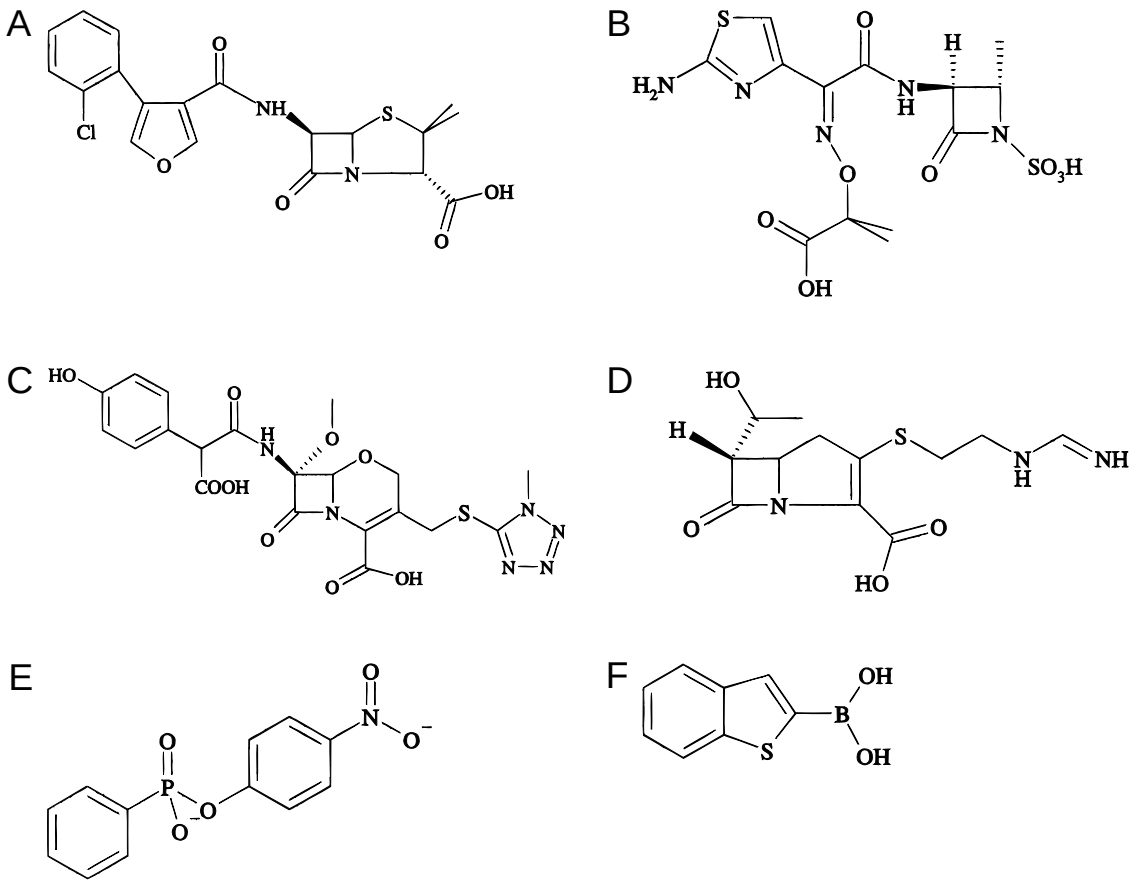

Fig. 3. Six inhibitors of AmpC β-lactamase: (**A**) cloxacillin; (**B**) aztreonam; (**C**) moxalactam; (**D**) imipenem (**A–D** are acylating inhibitors); (**E**) PNPP, an irreversible transition state analog; and (**F**) BZBTH2B, a reversible transition state analog.

monitored by near-UV CD, a measure of tertiary structure, and by fluorescence excitation. When monitored by near-UV CD at 270 nm, the T_m was 54.2 °C, and the ΔH_{VH} was 174 kcal/mol (Fig. 4B) (Table 1). These values closely resemble those returned by far-UV CD (Table 1). We note that the denaturation followed by near-UV CD was not fully reversible, presumably reflecting the relatively high concentration required for this low sensitivity technique (32–42 μg/mL vs. 5–13 μg/mL required in the far-UV CD). This denaturation, however, was reversible in 50 mM KPi, 800 mM KCl, 45% ethylene glycol. Under these conditions, the denaturation as followed by near-UV CD had a T_m of 49.3 °C and a ΔH_{VH} of 182 kcal/mol as compared to the far-UV CD, which had a T_m of 49.6 °C and ΔH_{VH} of 185 kcal/mol. Thus, the denaturation as followed by near-UV CD provides similar thermodynamic values as those observed with far-UV CD. When monitored by fluorescence excitation at 227 nm in our standard 38% ethylene glycol

Table 1. *Thermodynamic quantities determined by thermal denaturation of AmpC and Y150F*

	Technique	T_m (°C)	ΔH_{VH} (kcal/mol)	ΔS_u (kcal/mol•K)	$\Delta\Delta G_u$[a] (kcal/mol)
AmpC	Far-UV CD	54.6 ± 0.2	182 ± 9.3	0.56 ± 0.03	—
	Near-UV CD	54.2 ± 0.5	174 ± 39	0.56 ± 0.13	—
	Fluorescence	54.1 ± 0.5	183 ± 39	0.56 ± 0.12	—
Y150F	Far-UV CD	53.3 ± 0.1	215 ± 15	0.66 ± 0.04	−0.7 ± 0.1[b]

[a] Determined by the method of Schellman (Becktel & Schellman, 1987): $\Delta\Delta G_u = \Delta T_m \cdot \Delta S_{WT}$.
[b] A negative $\Delta\Delta G_u$ means a decrease in stability as indicated by a decrease in the T_m.

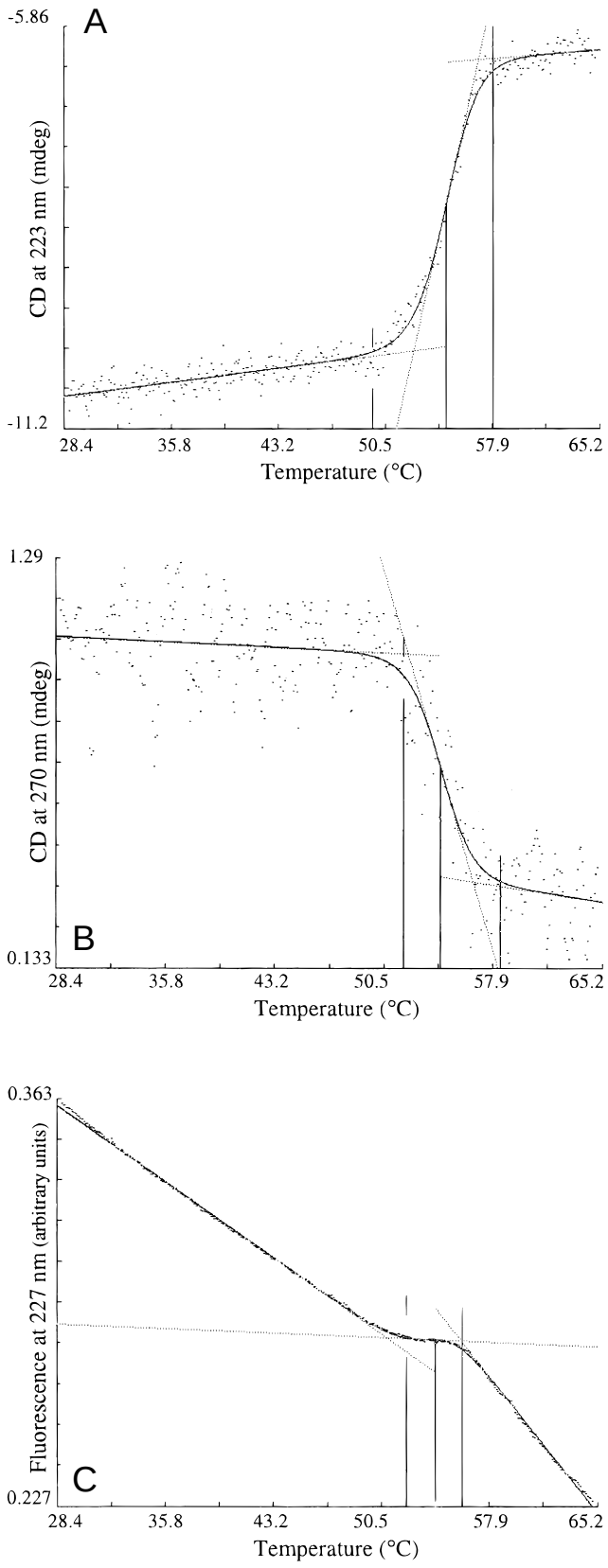

Fig. 4. Thermal denaturation of AmpC as monitored by various techniques as analyzed by EXAM. The dotted lines indicate asymptotes of the upper and lower baselines and the tangent to the profile at its midpoint; the solid line indicates the least-squares fit to the data (Kirchhoff, 1993). Values are given in Table 1. **A:** Far UV CD. **B:** Near-UV CD. **C:** Fluorescence.

buffer, the average T_m was 54.1 °C, and the average ΔH_{VH} was 183 kcal/mol (Fig. 4C) (Table 1). The denaturation was reversible as monitored by return of fluorescence signal after quick cooling.

The T_m and ΔH_{VH} values determined by thermal denaturation of AmpC appear to be independent of spectral technique. We note that the T_m values were slightly dependent on the rate of temperature increase; between 1.5–4 °C/min, the T_m increased monotonically (from 54.5 °C at a temperature ramp rate of 1.5 °C/min to 55.2 °C at a rate of 4 °C/min). Conversely, the ΔH_{VH} values did not vary, within the range of experimental error, as the ramp rate was altered. Taken together, these data suggest that AmpC denatures in a reasonable approximation to the reversible, two-state ideal.

AmpC Y150F was also denatured by temperature (Fig. 5). The T_m of this protein was reduced by 1.3 °C compared to AmpC WT, to 53.3 °C, with a ΔH_{VH} of 215 kcal/mol (Table 1). This suggests that AmpC Y150F is 0.7 kcal/mol less stable than WT. Upon quick cooling after denaturation, 87% of the folded CD signal returned.

Thermal denaturation with inhibitors

To assess noncovalent interaction energies, adducts of AmpC were denatured by temperature. AmpC WT in complex with cloxacillin was reversibly denatured by temperature (Fig. 6). Compared to AmpC alone, the T_m was increased by 5.8 °C, a stabilization of 3.2 kcal/mol (Table 2). Aztreonam also stabilized the complex; the T_m increased by 4.9 °C, equivalent to an increase in stability of 2.7 kcal/mol. AmpC WT in complex with moxalactam was also reversibly denatured by temperature (Fig. 6). In this case, the T_m was decreased by 3.2 °C, a destabilization of 1.8 kcal/mol. AmpC in complex with imipenem was reversibly denatured by temperature; the T_m was decreased by 1.2 °C, a destabilization of 0.7 kcal/mol (Table 2).

One concern we had was that the covalent enzyme-inhibitor adducts might break down over the course of the thermal denaturation. This would affect the resulting folding analyses. To investigate this question, we looked at the enzymatic activity of the

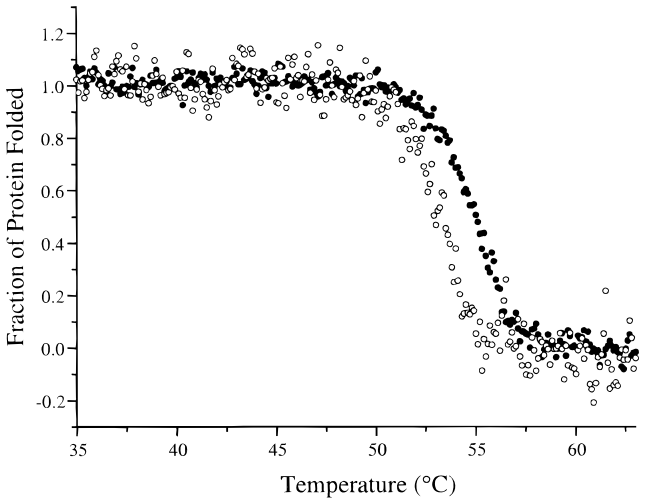

Fig. 5. Reversible, two-state thermal denaturation of AmpC and Y150F as monitored by far-UV CD at 223 nm. Values are given in Table 1. Solid circles indicate AmpC WT; open circles indicate AmpC Y150F.

Table 2. *Changes in the T_m and $\Delta\Delta G_u$ values of AmpC and Y150F when denatured in the presence of various inhibitors*

	AmpC WT (T_m = 54.6 °C; ΔH_{VH} = 182 kcal/mol)			AmpC Y150F (T_m = 53.3 °C; ΔH_{VH} = 215 kcal/mol)		
	ΔT_m (°C)	ΔH_{VH} (kcal/mol)	$\Delta\Delta G_u$[a] (kcal/mol)	ΔT_m (°C)	ΔH_{VH} (kcal/mol)	$\Delta\Delta G_u$[a] (kcal/mol)
+Cloxacillin	+5.8 ± 0.1	177 ± 11	+3.2 ± 0.2	−1.8 ± 0.1	184 ± 21	−1.2 ± 0.1
+Aztreonam	+4.9 ± 0.2	181 ± 3	+2.7 ± 0.2	N.D.[b]	N.D.	N.D.
+Moxalactam	−3.2 ± 0.1	200 ± 15	−1.8 ± 0.1	−4.0 ± 0.1	207 ± 39	−2.6 ± 0.2
+Imipenem	−1.2 ± 0.1	156 ± 6	−0.7 ± 0.07	N.D.	N.D.	N.D.
+PNPP	+2.5 ± 0.1	187 ± 11	+1.4 ± 0.1	−0.1 ± 0.2	194 ± 13	−0.1 ± 0.2
+BZBTH2B	+3.0 ± 0.2	181 ± 9	+1.7 ± 0.1	−0.1 ± 0.3	184 ± 56	−0.1 ± 0.3

[a] Determined by the method of Schellman (Becktel & Schellman, 1987): $\Delta\Delta G_u = \Delta T_m \cdot \Delta S_{\text{apo-enzyme}}$.
[b] Not determined.

enzyme-moxalactam mixture before thermal denaturation and then after denaturation and renaturation. Cephalothin, which is highly labile to uninhibited AmpC, was used as a substrate in these reactions. AmpC was highly and equally inhibited before denaturation and after renaturation. Since uninhibited AmpC is fully active after renaturation, this suggests that the adducts are stable to denaturation.

Complex formation with transition state analogs stabilized AmpC. The irreversible transition state analog, PNPP, increased the T_m by 2.5 °C, a stabilization of 1.4 kcal/mol (Table 2). BZBTH2B, a reversible transition state analog, increased the T_m by 3.0 °C, equivalent to a stabilization of 1.7 kcal/mol (Table 2).

AmpC Y150F was also denatured in the presence of these inhibitors. Cloxacillin decreased the T_m by 1.8 °C, a destabilization of 1.2 kcal/mol. Moxalactam decreased the T_m by 4.0 °C, a destabilization of 2.6 kcal/mol. There were no T_m changes when either PNPP or BZBTH2B was incubated with AmpC Y150F (Table 2).

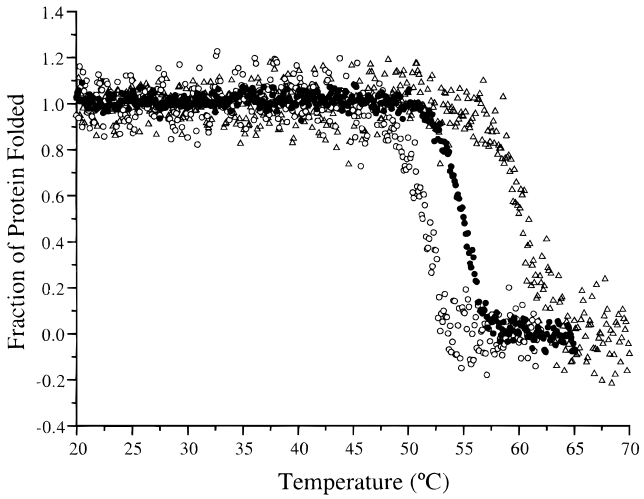

Fig. 6. Reversible, two-state thermal denaturation of AmpC WT alone, with moxalactam, and with cloxacillin as monitored by far-UV CD at 223 nm. Values are given in Table 2. Solid circles indicate AmpC WT. Open circles indicate AmpC with moxalactam. Open triangles indicate AmpC with cloxacillin.

Solvent denaturation

To further investigate two-state behavior, AmpC WT was reversibly denatured by Gdn·HCl in 50 mM KPi, 100 mM KCl, pH 6.8 buffer (Fig. 7A). The C_m was 1.43 M Gdn·HCl, the *m*-value was 9.8 kcal/mol M; the $\Delta G_u^{H_2O}$ was 14.0 kcal/mol (Table 3). The denatured samples fully refolded upon dilution.

AmpC Y150F was reversibly denatured by Gdn·HCl (Fig. 7B). Here, the C_m decreased to 1.32 M Gdn·HCl, and the *m*-value was 7.4 kcal/mol M. Using the average *m*-value method of Pace (1995), which is less sensitive to variations in the *m*-value and is considered more reliable, the $\Delta\Delta G_u^{H_2O}$ is thus −1.0 kcal/mol vs. AmpC WT (Table 3). This value compares to a $\Delta\Delta G_u$ of −0.7 kcal/mol determined by thermal denaturation.

AmpC WT in complex with the irreversible inhibitor PNPP was also denatured by Gdn·HCl (Fig. 7C). The C_m was increased to 1.56 M Gdn·HCl. The $\Delta\Delta G_u^{H_2O}$ is thus +1.2 kcal/mol vs. AmpC WT (Table 3). This compares to a $\Delta\Delta G_u$ of +1.4 kcal/mol determined by thermal denaturation.

The apparent monotonic relationship between $\Delta\Delta G_u$ values determined by thermal and solvent denaturation, and their close quantitative correspondence, are further evidence that thermodynamic quantities are being measured. Because these thermal and solvent denaturation experiments take place in different buffers and at different temperatures, we do not expect the $\Delta\Delta G_u$ values to correspond exactly.

Discussion

Complementarity of β-lactams and other ligands to AmpC

Some β-lactams bind to and significantly stabilize AmpC. This is true for cloxacillin and aztreonam, which have $\Delta\Delta G_u$ values of +3.2 and +2.7 kcal/mol, respectively. Surprisingly, some β-lactams bind to and significantly destabilize AmpC. Moxalactam and imipenem destabilize the enzyme by 1.8 and 0.7 kcal/mol, respectively. All four compounds are effective inhibitors of AmpC, but they have dramatically different effects on enzyme stability. What is the key to their inhibition of AmpC?

These β-lactams inhibit AmpC by forming a stable acyl adduct with the enzyme, blocking the active site. Although we think of

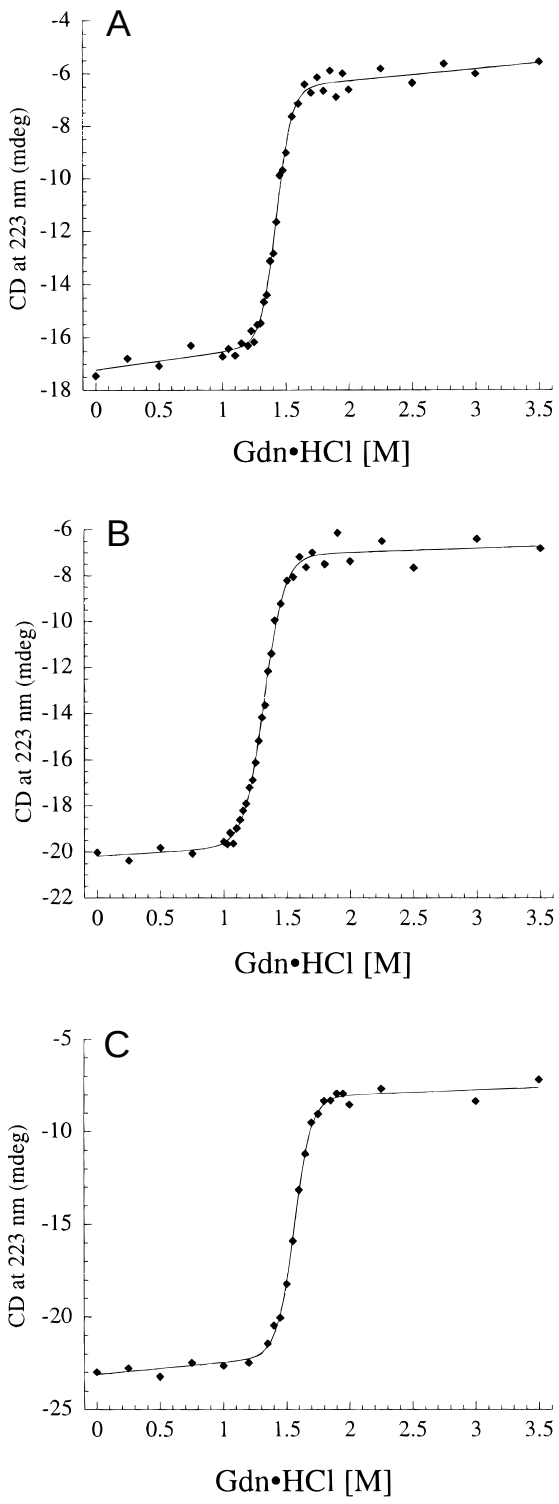

Fig. 7. Solvent denaturation of AmpC WT alone, AmpC Y150F alone, and AmpC WT with PNPP by Gdn·HCl at 25 °C. Values are given in Table 3. **A:** AmpC WT. **B:** AmpC Y150F. **C:** AmpC WT with PNPP.

inhibitors as forming favorable noncovalent interactions with their target enzymes, this need not be true for an inhibitor that acts covalently. The covalent bond between the enzyme and inhibitor is sufficient to halt the enzyme's action.

Given that the covalent bond is central in the inhibition of AmpC, it becomes clear that the secondary interactions, the noncovalent interactions, can be either favorable or unfavorable. The increase in thermodynamic stability that we see when AmpC binds β-lactams such as cloxacillin and aztreonam indicates that favorable noncovalent interactions between the inhibitor and the enzyme have formed. Conversely, moxalactam and imipenem form long-lived covalent adducts with AmpC, but their net noncovalent interactions with the enzyme are unfavorable. A covalent inhibitor can either stabilize or destabilize an enzyme. By studying the reversible denaturation of β-lactam-AmpC adducts, we can distinguish for the first time between covalent inhibitors that complement the binding site, and those that do not.

To what interactions can the destabilization caused by moxalactam and imipenem be attributed? Both have an unusual nonhydrogen substituent in the 6(7)α-position of the lactam ring; this is a methoxy in the case of moxalactam and an hydroxyethyl in the case of imipenem (Fig. 3). This is in contrast to prototypical β-lactams, which have a hydrogen in this position. The large α-face substituent may explain the destabilization of the complex. This suggestion is consistent with recent structural studies of the complex between the β-lactamase TEM-1 and imipenem (Maveyraud et al., 1998). In this structure, imipenem binds to TEM-1 in an unusual conformation, with the lactam carbonyl oxygen 3.7 Å from its normal location in the hydrolytic binding site (Fig. 8) (Strynadka et al., 1992; Maveyraud et al., 1998; Usher et al., 1998). In this conformation, several favorable interactions between the acyl adduct and the enzyme are lost. These include two hydrogen bonds between enzyme main-chain nitrogens and the lactam carbonyl oxygen of the adduct, which are conserved in every other serine β-lactamase-adduct structure. Bound imipenem presumably adopts this unusual configuration to avoid steric clashes between its 6α substituent and the enzyme that would occur if it bound in the canonical configuration. By forcing the acyl group to rotate out of the hydrolytic binding site, the 6α-hydroxyethyl group deactivates the imipenem adduct against hydrolytic attack (Maveyraud et al., 1998). A similar conformational change in AmpC would explain the lack of reactivity of the acyl adducts of moxalactam and imipenem and their destabilization of the enzyme.

If imipenem and moxalactam do adopt this unusual conformation in AmpC, it would explain why these β-lactams are good inhibitors (or poor substrates) of both class A and class C β-lactamases. It has been proposed that the 6(7)α substituents reduce the reactivity of the acyl adducts by displacing the hydrolytic water of class A β-lactamases, which comes from the α-face of the ring. However, in class C β-lactamases such as AmpC, the hydrolytic water is thought to attack from the opposite face of the β-lactam ring—the β-face (Bulychev et al., 1997). Both the structural data in class A β-lactamases and the thermodynamic data presented here suggest that the inhibition of these two classes of β-lactamases by 6(7)α-substituted β-lactams, such as imipenem and moxalactam, occurs by the same mechanism—displacement of the electrophilic acyl center from the point of hydrolytic attack.

The interactions of AmpC with two transition state analogs were also studied. In complex with both PNPP (Rahil & Pratt, 1994), an irreversible inhibitor, and BZBTH2B (Weston et al., 1998), a reversible inhibitor, AmpC was stabilized. This suggests that the enzyme's active site is complementary to the transition state of the reaction, as expected (Rahil & Pratt, 1994).

Table 3. *Thermodynamic quantities determined by solvent denaturation by Gdn·HCl*

	C_m (M)	*m*-value (kcal/mol M)	$\Delta G_u^{H_2O}$ [a] (kcal/mol)	$\Delta\Delta G_u^{H_2O}$ [b] (kcal/mol)
AmpC WT	1.43 ± 0.03	9.8 ± 0.8	14.0 ± 1.1	—
AmpC Y150F	1.32 ± 0.03	7.4 ± 0.5	9.7 ± 0.7	−1.0 ± 0.4
AmpC WT + PNPP	1.56 ± 0.04	8.6 ± 0.6	13.4 ± 1.0	−1.2 ± 0.5

[a] Determined by $\Delta G_u^{H_2O} = C_m \cdot m\text{-value}$.

[b] Determined by the method of Pace (1995): $\Delta\Delta G_u^{H_2O} = (C_{m_{WT}} - C_{m_{mut}}) \cdot [(m\text{-value}_{WT} + m\text{-value}_{mut})/2]$. Due to the variability in the *m*-values, this method is more reliable than $\Delta\Delta G_u^{H_2O}$ values determined by direct subtraction of $\Delta G_u^{H_2O}$ values.

The stability of Y150F and its adducts

A controversial aspect of the AmpC mechanism is the role of Tyr150. Substitution of this residue by a Phe reduces the activity of AmpC by 1,000–10,000-fold (Dubus et al., 1995), and the residue has been proposed to play a role in transition state recognition (Oefner et al., 1990; Lobkovsky et al., 1994). On the other hand, the hydrolysis of some β-lactams is only slightly affected by the Tyr to Phe substitution (Dubus et al., 1994), and other groups that might take the role of this residue in transition state stabilization have been proposed (Bulychev et al., 1997).

We found that the Y150F mutant enzyme is destabilized by cloxacillin, contrary to the stabilization seen in WT (Table 2). Compared to the WT adduct, the Y150F-cloxacillin adduct is destabilized by 4.4 kcal/mol. This suggests that Tyr150 is involved in the recognition of the acyl intermediate. Further clues to the role of Tyr150 come from the interactions between the Y150F mutant and the non-β-lactam inhibitors. Native AmpC is stabilized by both BZBTH2B, a reversible transition state analog (Weston et al., 1998), and PNPP, an irreversible transition state analog (Rahil & Pratt, 1994). Conversely, the Y150F enzyme is not stabilized by either compound, suggesting that the mutant enzyme interacts poorly with these two potent inhibitors. These results support earlier studies that show that Tyr150 is a key residue for the hydrolytic mechanism of AmpC, presumably by interacting with the transition state. Unexpectedly, our data suggest that Tyr150 also interacts, either directly or indirectly, with the acyl adduct ground state. In X-ray crystal structures of AmpC, Tyr150 forms hydrogen bonds with catalytic residues Lys67, Lys315, and Ser64 (Lobkovsky et al., 1993; Usher et al., 1998). This residue may help organize the AmpC active site.

Conclusions

Serine β-lactamases and PBPs play key roles in antibiotic resistance and antibiotic action and have been intensely studied. Because these enzymes form covalent intermediates with β-lactam substrates and inhibitors, the energetic complementarity of these enzymes for their cognate ligands is not well understood. The thermodynamic stability of AmpC β-lactamase in its bound and free forms allows us to determine the energetic complementarity of β-lactams for this enzyme. As expected, AmpC forms favorable noncovalent interactions with the β-lactams cloxacillin and aztreonam, which are widely used in antibiotic chemotherapy because of their stability to β-lactamases. AmpC also forms favorable noncovalent interactions with the transition state analogs PNPP and BZBTH2B. Unexpectedly, AmpC is destabilized by the "β-lactamase

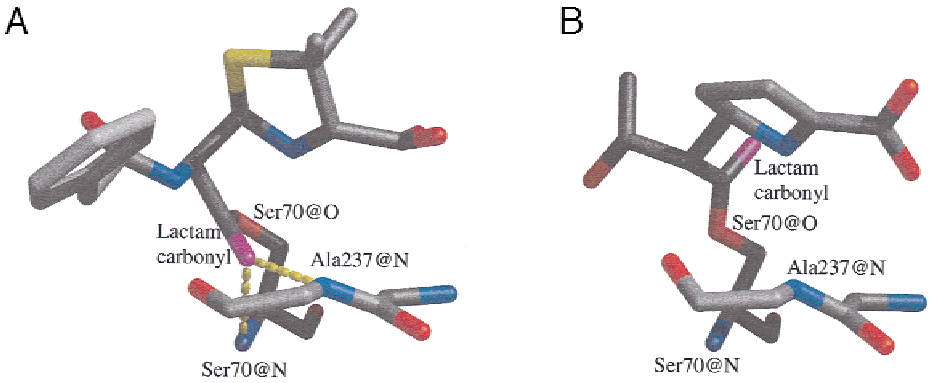

Fig. 8. Crystal structures of the acyl adducts between TEM-1 β-lactamase and (**A**) penicillin G (Strynadka et al., 1992) and (**B**) imipenem (Maveyraud et al., 1998). Carbon atoms are colored gray, oxygen atoms red, nitrogen atoms blue, and sulfur atoms yellow; in each figure, the lactam carbonyl oxygen is colored magenta. **A:** In the penicillin G-TEM-1 structure, the lactam carbonyl oxygen is bound in the hydrolytic binding site, making hydrogen bonds with the backbone nitrogens of Ser70 and Ala237. **B:** In the imipenem-TEM-1 structure, the imipenem has twisted so that the lactam carbonyl oxygen is now 3.7 Å from the position its prototypical position in the hydrolytic binding site. The R2 side chain of imipenem has been removed from this figure for clarity. This figure was generated using the MidasPlus display program (Ferrin et al., 1988).

stable" β-lactams moxalactam and imipenem, which are also widely used antibiotics because of their stability to β-lactamases. The ability of imipenem and moxalactam to resist hydrolytic deacylation may be because of their adoption of a strained conformation in the active site of the β-lactamase, which removes their electrophilic centers from the point of hydrolytic attack. Moxalactam and imipenem are good inhibitors because they are activated electrophiles; overall, they do not complement the enzyme.

The ability to reversibly denature AmpC provides an energetic component to the structure-function studies of this enzyme. It should be possible to measure the binding affinities of many β-lactams to AmpC or deacylation deficient mutant AmpC enzymes by determining changes in the melting temperatures. This would allow for structure-activity relationships that are based in energies of binding. It would also allow for an energy-based dissection of residue–ligand and residue–residue interactions, the latter of which speak to the internal stability of the enzyme. Similar studies may be useful for PBPs, which, like AmpC, are intensely studied because of their role as targets of antibiotic chemotherapy.

Materials and methods

Enzyme preparation

AmpC WT was expressed and purified as described (Usher et al., 1998). AmpC Y150F was made by oligonucleotide directed mutagenesis (Kunkel et al., 1987) and expressed using the same method as WT. To isolate the mutant enzyme, the *Escherichia coli* cells were resuspended in 10 mM Tris-HCl pH 7, lysed by sonication, and then ultracentrifuged. The supernatant was filtered and loaded onto an S-sepharose column previously equilibrated with 10 mM Tris-HCl. The protein was eluted with a 10–100 mM Tris-HCl gradient. The protein eluted at approximately 55 mM Tris-HCl. Protein concentration and purity were determined as described for wild-type (Usher et al., 1998). Unless otherwise indicated, each enzyme was studied at a concentration of 5–13 μg/mL.

Buffer preparation

Each buffer was prepared using ACS reagent grade potassium chloride (KCl) from Sigma Chemical (St. Louis, Missouri) and potassium phosphate (KPi) from Aldrich Chemical (Milwaukee, Wisconsin) in deionized water (MilliQ). The pH of each buffer was adjusted by dropwise addition of 3 N HCl or 10 N NaOH from Aldrich Chemical. Spectroscopic grade ethylene glycol from Sigma Chemical was also used. Ethylene glycol improved the reversibility of unfolding, presumably by reducing aggregation of the denatured state. Thermal denaturation took place in 50 mM KPi, 200 mM KCl, 38% ethylene glycol, pH 6.8, unless otherwise indicated. This percentage of ethylene glycol gave robust, apparently two-state, reversible thermal denaturation. Lower amounts of ethylene glycol reduced the reversibility of the thermal melts.

For solvent denaturation, stock solutions of 6.3 M guanidinium hydrochloride (Gdn·HCl) were made by addition of biotechnology grade Gdn·HCl from Amresco (Solon, Ohio) to 50 mM KPi, 100 mM KCl, pH 6.8 buffer, and readjustment of the pH to 6.8. The stock was kept at −20 °C until used. Denaturation buffers were prepared by adding the appropriate amount of 6.3 M Gdn·HCl stock to 50 mM KPi, 100 mM KCl, pH 6.8 to produce a given concentration of Gdn·HCl; there was no change in the buffer or salt concentrations. For renaturation, the sample was diluted twofold by addition of 50 mM KPi, 100 mM KCl, pH 6.8; reversibility was judged by the return of the folded CD signal at the appropriate wavelength.

CD measurements

CD experiments were carried out in a Jasco J-715 spectropolarimeter with a Jasco PTC-348WI peltier-effect temperature controller. Quartz cells with a 1 cm path length from Hellma (Jamaica, New York) were used for all experiments. For thermal denaturations, an in-cell temperature probe and stirbar were used. The program EXAM (Kirchhoff, 1993) was used to calculate all T_m and ΔH_{VH} values for the thermal denaturations. EXAM performs a least-squares fit of the two-state transition model, in which the two states of the protein are fully folded and fully unfolded (Kirchhoff, 1993). Error estimates are listed in the tables. In the EXAM analyses, the change in heat capacity upon denaturation (ΔC_p) for each enzyme is used as one fitting parameter; it was set to 6.0 kcal/mol K for each enzyme. Experimental determination of the ΔC_p for AmpC using thermal denaturation with various concentrations of Gdn·HCl was consistent with this value (data not shown). This ΔC_p value is also consistent with those methods based on the size and percent hydrophobicity of the enzyme (Dill et al., 1989). A ΔC_p value of 5.1 kcal/mol K was calculated using a method based on the number of amino acids in the enzyme (Myers et al., 1995). The ΔH_{VH} and T_m values are affected only slightly by varying the ΔC_p value, and the difference between 5.1 and 6.0 kcal/mol K alters insignificantly the calculated values of T_m, ΔH_{VH}, and ΔS_u. Solvent denaturations were analyzed using the program KaleidaGraph from Synergy Software (Reading, Pennsylvania).

Samples were monitored for helical content by CD in the far-UV region at 223 or 232 nm with the higher wavelength being used to reduce light absorption by ligand solutions; the behavior was identical at the two wavelengths. The samples were monitored for tertiary structure by CD in the near-UV region at 270 nm at an enzyme concentration of 32–42 μg/mL, a fourfold higher concentration than necessary for far-UV CD or fluorescence, owing to the low sensitivity of the near-UV CD. Thermal melting was performed at ramp rates of 2 °C/min unless otherwise indicated. Reversibility was judged using two criteria: the return of the original CD signal upon quick cooling and comparison of the enzyme's activity prior to denaturation and then after renaturation.

Incubation experiments with cloxacillin, moxalactam, PNPP from Sigma Chemical, aztreonam from ICN Pharmaceuticals (Costa Mesa, California), and imipenem were done by mixing the protein solution and the inhibitor (in 70–100-fold excess) in a microfuge tube. An aliquot of this incubation mixture was added to 3.5 mL of pre-equilibrated buffer solution; melting was performed as usual. For some ligands, acylation was slow; we report the largest reproducible ΔT_m, which occasionally demanded substantial pre-incubation (e.g., for PNPP, pre-incubation lasted three days). With BZBTH2B, from Lancaster Synthesis (Windham, New Hampshire) no pre-incubation was necessary; the enzyme and inhibitor were added simultaneously to the buffer solution; the final concentration of BZBTH2B was 28.4 μM. $\Delta\Delta G_u$ values were determined by the method of Schellman for all complexes of enzyme with inhibitor and also mutant enzymes (Becktel & Schellman, 1987):

$$\Delta\Delta G_u = \Delta T_m \cdot \Delta S_{\text{apo-enzyme}}. \quad (1)$$

In this study, increases in the T_m indicate stabilization, corresponding to a positive $\Delta\Delta G_u$ value, and decreases in the T_m indicate destabilization, giving a negative $\Delta\Delta G_u$ value.

Fluorescence measurements

Fluorescence experiments were performed in a Jasco J-715 spectropolarimeter with a peltier-effect temperature controller and an excitation fluorescence attachment. This allowed us to monitor thermal behavior by CD and fluorescence simultaneously. An in-cell temperature probe and stirbar were used. AmpC samples were excited at 227 nm. Thermal melting was performed as indicated for the CD measurements. Reversibility was judged by the return of the fluorescence signal upon quick cooling.

Solvent denaturations

AmpC, Y150F, and AmpC with PNPP were denatured with Gdn·HCl in 50 mM KPi, 100 mM KCl, pH 6.8 buffer at 25 °C. For AmpC with PNPP, the enzyme was incubated with the inhibitor for three days prior to solvent denaturation. For all three studies, separate buffer samples were prepared for each Gdn·HCl concentration in microfuge tubes. The appropriate enzyme or solution was added, and the samples were incubated at 25 °C for 24 h. The CD signal of the enzyme was measured at 223 nm. To determine $\Delta G_u^{H_2O}$, the Gibbs energy of unfolding at zero denaturant, and the m-value, the dependence of ΔG_u on Gdn·HCl concentration, the data were plotted in KaleidaGraph (Synergy Software) and analyzed using the Pace method (Pace, 1986) by a nonlinear least-squares fit to the following equation:

$$I = \frac{(m_f \cdot [D] + y_f) + (m_u \cdot [D] + y_u) \cdot \exp((-\Delta G_u^{H_2O} + m_{eq} \cdot [D])/RT)}{1 + \exp((-\Delta G_u^{H_2O} + m_{eq} \cdot [D])/RT)} \quad (2)$$

where I is the ellipticity; y_f, y_u, m_f, and m_u are the intercepts and slopes of the folded and unfolded baselines, respectively; m_{eq} is the m-value; and $[D]$ is the concentration of Gdn·HCl. Error estimates are listed in the tables. The values were used to calculate a midpoint concentration of denaturation (C_m) from the m-value and $\Delta G_u^{H_2O}$ (Pace, 1986):

$$\Delta G_u^{H_2O} = C_m \cdot m\text{-value}. \quad (3)$$

To determine $\Delta\Delta G_u$ values for both mutant AmpC and AmpC with inhibitors as compared to WT, the method of Pace was used (Pace, 1995):

$$\Delta\Delta G_u^{H_2O} = (C_{m_{WT}} - C_{m_{mut}}) \cdot [(m\text{-value}_{WT} + m\text{-value}_{mut})/2]. \quad (4)$$

Acknowledgments

This work was partly supported by MCB-9734484 from the NSF. We are grateful to N. Strynadka and S. Mobashery for sharing the structures of Pen-G/TEM-1 and imipenem/TEM-1, respectively. We thank the Keck Biophysics Facility for use of its equipment, Jesus Blazquez for imipenem, and Hector Rodriguez for help in six parameter fittings. We thank E. Silinsky, W. Anderson, F. Neuhaus, D. Lorber, and R. Powers for reading this manuscript. B.M.B. wishes to thank S.P.B. and B.R.B. for guidance in data analysis.

References

Becktel W, Schellman J. 1987. Protein stability curves. *Biopolymers 26*:1859–1877.

Bulychev A, Massova I, Miyashita K, Mobashery S. 1997. Nuances of mechanisms and their implications for evolution of the versatile beta-lactamase activity: From biosynthetic enzymes to drug resistance factors. *J Am Chem Soc 119*:7619–7625.

Christensen H, Martin M, Waley S. 1990. Beta-lactamases as fully efficient enzymes. Determination of all the rate constants in the acyl-enzyme mechanism. *Biochem J 266*:853–861.

Dill KA, Alonso DO, Hutchinson K. 1989. Thermal stabilities of globular proteins. *Biochemistry 28*:5439–5449.

Dubus A, Normark S, Kania M, Page MG. 1994. The role of tyrosine 150 in catalysis of β-lactam hydrolysis by AmpC β-lactamase from *Escherichia coli* investigated by site-directed mutagenesis. *Biochemistry 33*:8577–8586.

Dubus A, Normark S, Kania M, Page MG. 1995. Role of asparagine 152 in catalysis of β-lactam hydrolysis by *E. coli* AmpC β-lactamase studied by site-directed mutagenesis. *Biochemistry 34*:7757–7764.

Ferrin TE, Huang CC, Jarvis LE, Langridge R. 1988. The MIDAS display system. *J Mol Graph 6*:13–27.

Fisher J, Belasco JG, Khosla S, Knowles JR. 1980. Beta-lactamase proceeds via an acyl-enzyme intermediate. Interaction of the *E. coli* RTEM enzyme with cefoxitin. *Biochemistry 19*:2895–2901.

Hall A, Knowles JR. 1976. Directed selective pressure on a beta-lactamase to analyze molecular changes involved in development of enzyme function. *Nature 264*:803–804.

Ishiguro M, Tanaka R, Namikawa K, Nasu T, Inoue H, Nakatsuka T, Oyama Y, Imajo S. 1997. 5,6-*Cis*-penems: Broad-spectrum antimethicillin-resistant *Staphylococcus aureus* beta-lactam antibiotics. *J Med Chem 40*:2126–2132.

Kirchhoff W. 1993. EXAM: A two-state thermodynamic analysis program. Gaithersburg, Maryland: NIST.

Kunkel TA, Roberts JD, Zakour RA. 1987. Rapid and efficient site-specific mutagenesis without phenotypic selection. *Methods Enzymol 154*:367–382.

Li N, Rahil J, Wright ME, Pratt RF. 1997. Structure-activity studies of the inhibition of serine beta-lactamases by phosphonate mono-esters. *Bioorg Med Chem 5*:1783–1788.

Lobkovsky E, Billings EM, Moews PC, Rahil J, Pratt RF, Knox JR. 1994. Crystallographic structure of a phosphonate derivative of the *Enterobacter cloacae* P99 cephalosporinase: Mechanistic interpretation of a beta-lactamase transition state analog. *Biochemistry 33*:6762–6772.

Lobkovsky E, Moews PC, Liu H, Zhao H, Frere JM, Knox JR. 1993. Evolution of an enzyme activity: Crystallographic structure at 2 resolution of cephalosporinase from the ampC gene of *E. cloacae* P99 and comparison with a class A penicillinase. *Proc Natl Acad Sci USA 90*:11257–11261.

Maveyraud L, Mourey L, Kotra LP, Pedelacq J, Guillet V, Mobashery S, Samama J. 1998. Structural basis for clinical longevity of carbapenem antibiotics in the face of challenge by the common class A beta-lactamases from the antibiotic-resistant bacteria. *J Am Chem Soc 120*:9748–9752.

Morton A, Matthews BW. 1995. Specificity of ligand binding in a buried nonpolar cavity of T4 lysozyme: Linkage of dynamics and structural plasticity. *Biochemistry 34*:8576–8588.

Myers JK, Pace CN, Scholtz JM. 1995. Denaturant *m* values and heat capacity changes: Relation to changes in accessible surface areas of protein unfolding. *Protein Sci 4*:2138–2148.

Oefner C, D'Arcy A, Daly JJ, Gubernator K, Charnas RL, Heinze I, Hubschwerlen C, Winkler FK. 1990. Refined crystal structure of beta-lactamase from *Citrobacter freundii* indicates a mechanism for beta-lactam hydrolysis. *Nature 343*:284–288.

Pace CN. 1986. Determination and analysis of urea and guanidine hydrochloride denaturation curves. *Methods Enzymol 131*:266–280.

Pace CN. 1995. Evaluating contribution of hydrogen bonding and hydrophobic bonding to protein folding. *Methods Enzymol 259*:538–554.

Rahil J, Pratt RF. 1994. Characterization of covalently bound enzyme inhibitors as transition state analogs by protein stability measurements: Phosphonate mono-ester inhibitors of a beta-lactamase. *Biochemistry 33*:116–125.

Schellman JA. 1976. The effect of binding on the melting temperature of biopolymers. *Biopolymers 15*:999–1018.

Strominger JL, Tipper DJ. 1965. Bacterial cell wall synthesis and structure in relation to the mechanism of action of penicillins and other antibacterial agents. *Am J Med 39*:708–721.

Strynadka NC, Adachi H, Jensen SE, Johns K, Sielecki A, Betzel C, Sutoh K, James MN. 1992. Molecular structure of the acyl-enzyme intermediate in beta-lactam hydrolysis at 1.7 resolution. *Nature 359*:700-705.

Usher KC, Blaszczak LC, Weston GS, Shoichet BK, Remington SJ. 1998. Three-dimensional structure of AmpC beta-lactamase from *E. coli* bound to a transition state analogue: Possible implications for the oxyanion hypothesis and for inhibitor design. *Biochemistry 37*:16082–16092.

Weston GS, Blazquez J, Baquero F, Shoichet BK. 1998. Structure-based enhancement of boronic acid-based inhibitors of AmpC beta-lactamase. *J Med Chem 41*:4577–4586.